Disease and Diagnosis

Dis Diagn. 2023; 12(4):161-167

doi 10.34172/ddj.2023.450

Original Article

Determining the Synergistic Effect of Magnetic Fields on the Induction of Apoptosis by Folic Acid Targeted Iron Superparamagnetic Nanoparticles Loaded With Lomustine on U87-MG Cell Line

Zeinolabedin Shrifian Dastjerdi[1,2], Elias Kargar Abargouei[1], Fahimeh Zamani Rarani[3], Ebrahim Eftekhar[2], Mohammad Zamani Rarani[1,2*], Dariush Hooshyar[1], Reza Afzalipour[4,2]

[1]Department of Anatomical Sciences, Medical School, Hormozgan University of Medical Sciences, Bandar Abbas, Iran
[2]Molecular Medicine Research Center, Hormozgan Health Institute, Hormozgan University of Medical Science, Bandar Abbas, Iran
[3]Department of Anatomical Sciences, School of Medicine, Isfahan University of Medical Sciences, Isfahan, Iran
[4]Department of Radiology, Faculty of Para-Medicine, Hormozgan University of Medical Sciences, Bandar Abbas, Iran

***Correspondence to**
Mohammad Zamani Rarani,
Email: mz123esf@gmail.com

Abstract

Background: Brain cancer is recognized as one of the deadliest cancers due to late detection and limitations of therapies. Glioblastoma occurs in different parts of the central nervous system and is the second leading cause of cancer death in people. There are many problems for the treatment of cancer cells. One of the limiting factors is the resistance of cancer cells to chemotherapy drugs. The use of nanoparticles (NPs) is an effective method for overcoming this problem.

Materials and Methods: Fe_3O_4 NPs were synthesized, and the size and morphology of NPs were determined by transmission electron microscopy, X-ray photoelectron spectroscopy, and Dynamic Light Scattering. The U87-MG cell line was cultured in Dulbecco's modified Eagle medium and treated with nano, nano-lomustine, lomustine, and complex with/without magnetic fields. Finally, half maximal inhibitory concentration (IC_{50}), MTT assay, and caspase8 and caspase9 expression were evaluated, and the data were analyzed with SPSS software.

Results: Our results demonstrated that cell apoptosis increased in lomustine and complex groups, especially with the magnetic field ($P>0.05$). Based on caspase9 expression analysis, this rate was increased with the magnetic field vs. its absence ($P>0.05$).

Conclusion: These findings indicated that a magnetic field, in addition to reducing the effective dose of lomustine, affects apoptosis with a change in the expression of genes involved in this process.

Keywords: Glioblastoma, Nanoparticle, Apoptosis, Caspase, Magnetic field

Received: September 13, 2022, **Accepted:** March 4, 2023, **ePublished:** 24 April, 2023

Introduction

In recent years, cancer has been recognized as one of the main causes of death in the world, and it has widely been spread in Iran during different ages (1). Among all types of cancer, brain cancer is one of the most deadly cancers due to late diagnosis and the limitations of conventional treatment methods, and its proper treatment remains an unsolved problem (2). The research conducted in this field has shown that approximately 82% of brain glioma tumors are glioblastoma multiform in terms of histopathology. Despite many efforts in the field of diagnosis and treatment, this type of cancer still has an extremely poor prognosis (3). Currently, the usual treatment for this type of cancer consists of surgery followed by fractional radiotherapy, along with chemotherapy. Despite many advances in the field of brain tumor surgery, it is impossible to remove all cancer cells for various reasons. Cancer cells remaining in the tumor bed after surgery and their rapid growth cause treatment failure and tumor recurrence. Radiotherapy and chemotherapy are used to destroy the remaining cells. Although this work increases the survival of patients with this cancer after surgery, for various reasons, the clinical results are not favorable (4, 5). Factors limiting the effect of chemotherapy and radiotherapy should be removed to achieve the desired results. One of the limiting factors is the resistance of cancer cells to radiotherapy and chemotherapy and insufficient doses of chemotherapy drugs and the effectiveness of these drugs (6). Various methods have been proposed to eliminate radiation

resistance and increase drug delivery to cancer cells, and research on such methods is ongoing (7). The use of superparamagnetic nanoparticles (NPs) is considered an effective technique in this field (8). Superparamagnetic NPs can play an important role in the treatment of cancer cells in the brain due to the radiation sensitization effect, on the one hand, and the ability to carry various drugs, on the other hand (7). Lomustine is one of the chemotherapy drugs that is widely employed to treat brain cancers. With the method of administration and the usual dose, the amount of this drug is extremely low in cancer cells. The complete destruction of cancer cells requires high doses of this drug and ionizing radiation, causing damage to healthy tissues and side effects (9, 10).

By using targeted superparamagnetic NPs carrying lomustine, it is possible to increase the amount of drug uptake in cancer cells while taking advantage of their radio-sensitizing properties. Targeting superparamagnetic NPs with folic acid is known as an effective method to increase the uptake of these NPs by cancer cells (11). The combination of two factors, namely, magnetic field and medicine, can cause synergy in killing cancer cells, and it can stop the growth of cancer cells with the usual doses of radiation and chemotherapy drugs while reducing the side effects of these factors (12, 13). Although the effect of magnetic fields on human tissues has not been well defined yet (14), its effect on increasing the activity and persistence, and concentration of free radicals has been proven previously (15). In addition, the magnetic field causes a large number of tumor cells to stay in the G2/M phase of the cell cycle, and this state increases their sensitivity to X-rays. Further, the genome repair processes are disrupted in the presence of the magnetic field (16).

Studies on iron oxide (FeO) superparamagnetic particles and various brain cancer cell lines have demonstrated that these particles will not only increase the contrast of magnetic resonance imaging (MRI) but can also carry drugs into the cells (17, 18).

In another study, FeO superparamagnetic particles with heat shock protein 70 were used against rat brain tumors. The pre-apoptotic effects of these particles were measured, and the results showed the potential of these particles in increasing cell death, targeted drug delivery, and the contrast of MRI images (19).

Similarly, another study investigated the colloidal stability of superparamagnetic FeO particles activated with carboxyl amine and the quantum effects of these particles on the induction of hyperthermia in cancer tissues and cell death, and the results were successful in these cases (20).

According to the provided explanations, this study intended to evaluate the synergistic effect of the magnetic field on the apoptotic properties of the targeted FeO NP complex with folic acid carrying lomustine, especially in relation to the expression of genes involved in apoptosis.

Materials and Methods

Cell Culture, Drug, and Treatment

The U87-MG cell line was obtained from the Pastor Institute of Animals Cell Culture. The cells were maintained in Dulbecco's modified Eagle medium (DMEM/F12) with 10% fetal bovine serum, 100 U/mL penicillin, and 100 µg/mL streptomycin and kept at 37˚C in a humidified atmosphere with 5% CO_2. For experiments, the cells were seeded in culture flasks after trypsinization (Trypsin-EDTA). Lomustine was purchased from Sigma-Aldrich Company (L5918) and dissolved in DMSO for appropriate concentrations according to the half maximal inhibitory concentration (IC_{50}) assay. After the cells were > 80% confluent and growing exponentially in the T75 culture flask, 10^6 U87-MG cells were counted and plated in the T75 culture flask and kept in a culture medium for 24 hours. Then, they were incubated with certain concentrations of NP based on the IC_{50} concentration, and the tests were performed at certain times (24, 48, and 72 hours).

Half Maximal Inhibitory Concentration Assay

The IC_{50} values for the lomustine in U87-MG cells were acquired after 24 hours of treatment. Briefly, 10^4 cells (U87-MG) were counted and placed into each well of a 12-well plate and were then treated with various lomustine concentrations for 24 hours. Next, 3(4, 5-dimethylthiazol-2-yl) 2, 5- diphenyl-tetrazolium bromide (MTT) survival assay was performed for evaluating cell viability with different drug concentrations in each group. A graph of cell viability versus drug concentration was used to calculate IC_{50} values for the U87-MG cell line.

Real-time Polymerase Chain Reaction

Total RNA from cells was extracted at the indicated times using the total RNA extraction kit and following the manufacturer's instructions (Yekta Tajhiz Azma, Tehran, Iran). After treatment with DNase I, Total RNA (100 ng) was reverse-transcribed to cDNA by using the Revert Aid™ First Strand cDNA Synthesis Kit (Yekta Tajhiz Azma, Tehran, Iran) according to the manufacturer's instructions. The SYBR Green quantitative PCR (qPCR) master mix kit (Yekta Tajhiz Azma, Tehran, Iran) was employed for real-time polymerase chain reaction (RT-PCR). Primer sequences are provided in Table 1. RT-PCRs were performed with StepOnePlus™ (Applied Biosystems). The program of RT-PCR consisted of 10 minutes at 95 ˚C followed by 40 cycles of the denaturation step at 95˚C for 15 seconds, followed by annealing and extension for 1 minute at 60˚C. Data were analyzed by the comparative Ct (ΔΔct) method. The relative expression levels of the genes were calculated by determining a ratio between the amount of every gene expression and that of endogenous control. Melting curve analysis (60˚C → 95˚C increment of 0.3˚C) was used to determine the melting temperature

of specific amplification products and primer dimmers. These experiments were conducted in triplicate and were independently repeated at least 3 times.

3(4, 5-Dimethylthiazol-2-yl) 2, 5-diphenyl-tetrazolium Bromide Assay

Overall, 10^4 cells per well were plated into 24-well plates. After 24 hours, the medium was removed, followed by adding drugs that were dissolved in the medium at certain concentrations. At the determined time points (24, 48, and 72 hours), cell viability was measured using MTT in the Dulbecco's Modified Eagle Medium (DMEM) for 3 hours. After lysis with DMSO, 100 µL aliquot of the soluble fraction was transferred into 96 well plates, and the optical density (OD) was computed with the plate reader system. The percentage of cells that were stained by MTT was determined by comparing the OD of each sample with that of the control group.

Flowcytometry Assay

The percentage of apoptotic cells was calculated by flowcytometry following Annexin V (FL1-H) and PI (FL2-H) labeling. A minimum of 4×10^5 cells/mL were analyzed for each sample. Cells that were treated in 24, 48, and 72 hours were washed in phosphate-buffered saline and resuspended in the binding buffer (1×, 5 µL). Annexin V-FITC was added to 195 µL cell suspensions, and then analysis was performed according to the manufacturer's protocol (Annexin V-FITC, eBioscience, USA). Finally, the apoptotic cells were counted by FACScan flowcytometry (Becton Dickinson, Heidelberg, Germany). These experiments were conducted in triplicate and were separately repeated at least 3 times.

Statistical Analysis

All the quantitative data were presented as the mean ± standard deviation. One-way analysis of variance, Tukey's post hoc test, and independent t-test were performed to determine the statistical significance among different groups by using SPSS software (version 26), and the significance level was accepted at $P<0.05$.

Results

Half Maximal Inhibitory Concentration Assay

In this assay, after the treatment of U87-MG cells with the MTT solution, the dark blue Formosan crystals were detected in viable cells, indicating their metabolic activity. The reduction in the number of cells directly relied on drug doses as represented by the IC_{50} in Figure 1. The IC_{50} values for the lomustine were determined (Figure 1), and the results revealed that the essential lomustine concentration to achieve the IC_{50} in U87-MG cells at 24 hours was 70 µM (Figure 1).

Table 1. Primers Used in the Real-Time Polymerase Chain Reaction

Primer	Sequence
Caspase8 forward	GGATGGCCACTGTGAATAACTG
Caspase8 reverse	TCGAGGACATCGCTCTCTCA
GAPDH forward	CACCACCATGGAGAAGGCTGG
GAPDH reverse	CCAAAGTTGTCATGGATGACC
Caspase9 forward	TGTCCTACTCTACTTTCCCAGGTTTT
caspase9 reverse	GTGAGCCCACTGCTCAAAGAT

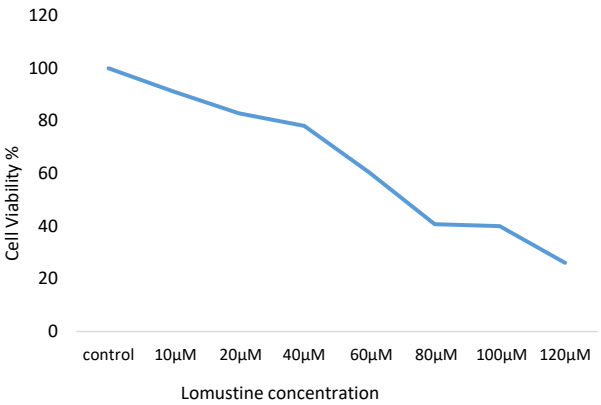

Figure 1. IC_{50} Assay for IC_{50} Analysis of Lomustine (Figure 1) in U87-MG Cancer Cell Lines. *Note*. IC_{50}: Half maximal inhibitory concentration; MTT: 3(4, 5-dimethylthiazol-2-yl) 2, 5-diphenyl-tetrazolium bromide. Cells were incubated with/without the drug at different concentrations, and the relative amount of viable cells was estimated by measuring the absorbance of the MTT solution. The graph of viability versus drug concentration was used to calculate IC_{50} values.

3(4, 5-Dimethylthiazol-2-yl) 2, 5-diphenyl-tetrazolium Bromide Cell Proliferation Assay

The effect of lomustine on cell proliferation was studied by using the MTT proliferation assay in the U87-MG cell line. To determine changes in the number of cells in the wells during the experiment, cell proliferation had to be measured 24, 48, and 72 hours after the treatment period (Figure 2). lomustine treatment on U87-MG cells showed lower OD at IC_{50} concentrations than controls, especially after 72 hours ($P>0.05$).

Flowcytometry

The flowcytometry assay was employed to determine the apoptotic potential of lomustine. Our results revealed that the 70 µM concentration of lomustine based on the IC_{50} concentration at the intended times (24, 48, and 72 hours) could significantly induce apoptosis in U87-MG cells, and it was increased with the magnetic field ($P>0.05$, Figure 3). Lomustine treatment arrested U87-MG cell proliferation and induced apoptosis (≥65% of inhibition) after 72 hours (Figure 3), and the apoptotic cell rate decreased in comparison with the control group cells, especially after 72 hours ($P<0.05$). DMSO that was

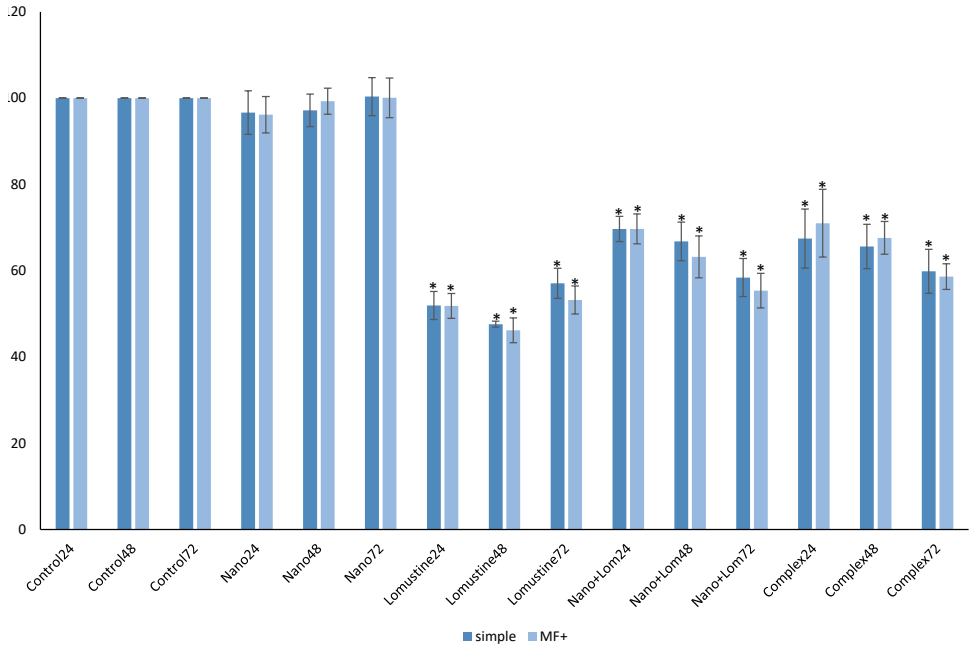

Figure 2. MTT Proliferation Assay at IC_{50} Concentrations 24, 48, and 72 Hours After Treatment. *Note*. MTT: 3(4, 5-dimethylthiazol-2-yl) 2, 5-diphenyl-tetrazolium bromide; IC_{50}: Half maximal inhibitory concentration. The growth rates decreased in the treated cells with Lomustine-loaded nanoparticles with/without magnetic fields as compared with untreated cells.

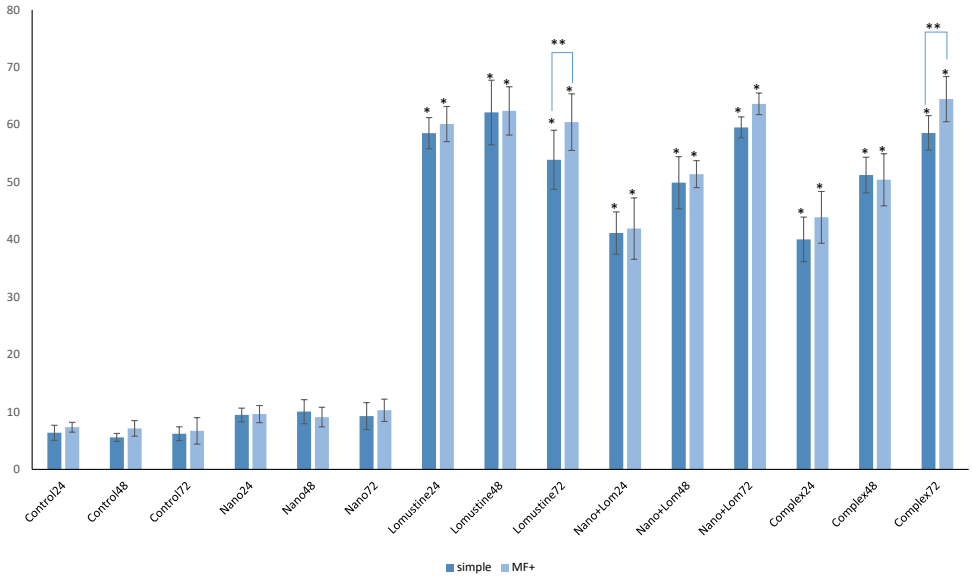

Figure 3. Relative Levels of Apoptotic Cells in U87-MG Cancer Cell Lines Treated With 70 μM Lomustine With/Without Magnetic Fields at Different Times. *Note*. Untreated cells were used to control groups.

used in the control sample (the drug vehicle) had a small amount of apoptosis in U87-MG cells than the control at different times ($P < 0.05$, Figure 3).

Results of Real-time Polymerase Chain Reaction

Real-time qPCR was utilized to examine lomustine effects (based on the IC_{50}) at different times on caspase8 and caspase9 gene expression in U87-MG cells. The expression of these genes was dramatically up-regulated by lomustine treatment with an ascending time manner, and in particular, it significantly increased 72 hours after treatment and under the magnetic field (Figure 3, $P < 0.05$, Figure 4).

Discussion

The application of FeO superparamagnetic NPs has been proposed as a new solution for imaging and treating tumors, especially brain tumors (21). Providing a surface that can be loaded with drugs, can accumulate at the tumor site, improve the quality of imaging, and facilitate

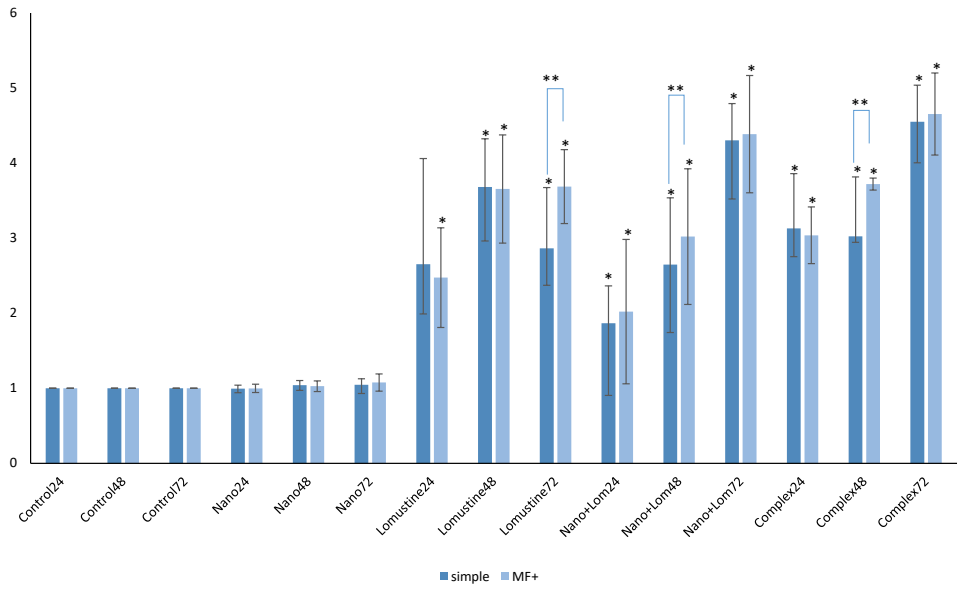

Figure 4. Effects of Lomustine on the Levels of Caspase8 and Caspase9 Expressions in U87-MG Cells 24, 48, and 72 Hours After Treatment With/Without the Magnetic Field. *Note*. This gene expression was up-regulated with lomustine treatment, especially with the magnetic field 72 hours after treatment ($P>0.05$).

the entry of the drug into the desired cells, and produce free radicals at the tumor site during radiotherapy, conductivity, and heat production in cancer cells when placed in the magnetic field, is only one of the studies conducted based on the properties of these materials (22).

The result of this study demonstrated that the simultaneous use of targeted drug-carrying NPs with a magnetic field has more apoptotic effects than the absence of a magnetic field. Some recent studies have confirmed the sensitivity of the genome to the magnetic field and the control of processes such as DNA synthesis and repair and gene expression by enzymes with the core of metal elements such as magnesium, calcium, and zinc under the effect of the magnetic field (23-25). It seems that the presence of a magnetic field can prevent the repair process of damaged DNA as a result of anticancer agents such as lomustine. In this regard, studies have shown that the magnetic field has clinical potential to control the growth of breast cancer cells (26). Moreover, the antitumor properties of the field in neuroblastoma and nephroblastoma (27) and the effect of stimulating apoptosis and reducing the viability of melanoma cancer cells (28) have also been confirmed under the influence of a magnetic field.

Several studies have been conducted regarding the mechanism of the effect of the magnetic field on the process of apoptosis; however, biological pathways related to this field have not been well defined yet (29). Studies have reported that the magnetic field of 6 mT by changing the amount of calcium ions increases the expression of genes involved in apoptosis (i.e., *p53* and *Bax*), while it decreases the expression of *bcl2* and *hsp70* genes, thereby affecting the amount of apoptosis in lymphocyte cells. It works both in vivo and in freshly isolated cells from the blood (30). The results of the mentioned study are consistent with those of the present study, indicating that the magnetic field increases the expression of *casp8* and *casp9* genes. It has also been confirmed that the magnetic field in in vivo and in vitro environments causes P53 stability and increases miR-34 expression by inhibiting iron metabolism in lung cancer cells. The molecular pathway of P53-miR 34a-E2F1/E2F3 inhibits cell proliferation and arrests the cell cycle and senescence of cells (31), and these results are in line with the findings of our study on increasing the expression of *casp8* and *casp9*, decreasing cell viability, and increasing cell apoptosis.

Lomustine is widely used for the treatment of brain neoplasms; however, due to many side effects, its use is limited to the dose, and this itself causes cell resistance (32).

Recent research has indicated that lomustine initiates cell death by activating genes involved in apoptotic pathways (33). *P16* is one of the key genes in the induction of apoptosis by some chemotherapy drugs such as cisplatin and lomustine (33). Lomustine inhibits cell proliferation through G2/M cell cycle arrest and increases the expression of P16, which binds to CDK4 and CDK6 and inhibits cyclin D to arrest the cell cycle (34), which conforms to the results of this study. Conducting a similar study in laboratory animals can provide more accurate and practical results and show the possible side effects of the targeted NP complex carrying lomustine.

Conclusion

The findings of this study revealed that using lomustine in the U87-MG cell line as a complex of targeted FeO NPs

with folic acid and the simultaneous use of a magnetic field increased apoptotic effects with the increased expression of caspases genes in addition to reducing the effective dose of lomustine and subsequently reducing its side effects.

Acknowledgements
We would like to appreciate the Central Laboratory Staff of Hormozgan Medical University for collaboration.

Authors' Contribution
Conceptualization: Mohammad Zamani Rarani, Reza Afzalipour, and Dariush Hooshyar.
Data curation: Dariush Hooshyar, Elias Kargar Abargouei.
Formal analysis: Mohammad Zamani Rarani.
Funding acquisition: Mohammad Zamani Rarani,Dariush Hooshyar
Investigation: Zeinolabedin Sharifian Dastjerdi, Elias Kargar Abargouei, Dariush Hooshyar.
Methodology: Zeinolabedin Sharifian Dastjerdi, Elias Kargar Abargouei, Mohammad Zamani Rarani.
Project administration: Mohammad Zamani Rarani**.**
Resources: Dariush Hooshyar, Elias Kargar Abargouei.
Supervision: Ebrahim Eftekhar, Reza Afzalipour.
Validation: Zeinolabedin Sharifian Dastjerdi, Elias Kargar Abargouei, Fahimeh Zamani Rarani.
Visualization: Dariush Hooshyar.
Writing–original draft: Fahimeh Zamani Rarani, Ebrahim Eftekhar, Dariush Hooshyar.
Writing–review & editing: Zeinolabedin Sharifian Dastjerdi, Elias Kargar Abargouei.

Competing Interests
The authors declared no conflict of interests related to this article.

Ethical Approval
This study was approved by the Ethics Committee of Hormozgan University of Medical Sciences (IR.HUMS.REC.1397.194).

Funding
This study was financially supported by Hormozgan University of Medical Sciences.

Informed Consent
Informed consent was obtained from all individual participants who attended the study.

References
1. Rezapour A, Nargesi S, Mezginejad F, Rashki Kemmak A, Bagherzadeh R. The economic burden of cancer in Iran during 1995-2019: a systematic review. Iran J Public Health. 2021;50(1):35-45. doi: 10.18502/ijph.v50i1.5070.
2. Alemany M, Velasco R, Simó M, Bruna J. Late effects of cancer treatment: consequences for long-term brain cancer survivors. Neurooncol Pract. 2021;8(1):18-30. doi: 10.1093/nop/npaa039.
3. Herrera-Oropeza GE, Angulo-Rojo C, Gástelum-López SA, Varela-Echavarría A, Hernández-Rosales M, Aviña-Padilla K. Glioblastoma multiforme: a multi-omics analysis of driver genes and tumour heterogeneity. Interface Focus. 2021;11(4):20200072. doi: 10.1098/rsfs.2020.0072.
4. Thakkar JP, Dolecek TA, Horbinski C, Ostrom QT, Lightner DD, Barnholtz-Sloan JS, et al. Epidemiologic and molecular prognostic review of glioblastoma. Cancer Epidemiol Biomarkers Prev. 2014;23(10):1985-96. doi: 10.1158/1055-9965.epi-14-0275.
5. Batash R, Asna N, Schaffer P, Francis N, Schaffer M. Glioblastoma multiforme, diagnosis and treatment; recent literature review. Curr Med Chem. 2017;24(27):3002-9. doi: 10.2174/0929867324666170516123206.
6. Hanif F, Muzaffar K, Perveen K, Malhi SM, Simjee Sh U. Glioblastoma multiforme: a review of its epidemiology and pathogenesis through clinical presentation and treatment. Asian Pac J Cancer Prev. 2017;18(1):3-9. doi: 10.22034/apjcp.2017.18.1.3.
7. Rick J, Chandra A, Aghi MK. Tumor treating fields: a new approach to glioblastoma therapy. J Neurooncol. 2018;137(3):447-53. doi: 10.1007/s11060-018-2768-x.
8. Játiva P, Ceña V. Use of nanoparticles for glioblastoma treatment: a new approach. Nanomedicine (Lond). 2017;12(20):2533-54. doi: 10.2217/nnm-2017-0223.
9. Jakobsen JN, Urup T, Grunnet K, Toft A, Johansen MD, Poulsen SH, et al. Toxicity and efficacy of lomustine and bevacizumab in recurrent glioblastoma patients. J Neurooncol. 2018;137(2):439-46. doi: 10.1007/s11060-017-2736-x.
10. Song J, Xue YQ, Zhao MM, Xu P. Effectiveness of lomustine and bevacizumab in progressive glioblastoma: a meta-analysis. Onco Targets Ther. 2018;11:3435-9. doi: 10.2147/ott.s160685.
11. Narmani A, Rezvani M, Farhood B, Darkhor P, Mohammadnejad J, Amini B, et al. Folic acid functionalized nanoparticles as pharmaceutical carriers in drug delivery systems. Drug Dev Res. 2019;80(4):404-24. doi: 10.1002/ddr.21545.
12. Zhang H, Liu XL, Zhang YF, Gao F, Li GL, He Y, et al. Magnetic nanoparticles based cancer therapy: current status and applications. Sci China Life Sci. 2018;61(4):400-14. doi: 10.1007/s11427-017-9271-1.
13. Farzin A, Etesami SA, Quint J, Memic A, Tamayol A. Magnetic nanoparticles in cancer therapy and diagnosis. Adv Healthc Mater. 2020;9(9):e1901058. doi: 10.1002/adhm.201901058.
14. Suhariningsih, Winarni D, Husen SA, Khaleyla F, Putra AP, Astuti SD. The effect of electric field, magnetic field, and infrared ray combination to reduce HOMA-IR index and GLUT 4 in diabetic model of Mus musculus. Lasers Med Sci. 2020;35(6):1315-21. doi: 10.1007/s10103-019-02916-z.
15. Okano H. Effects of static magnetic fields in biology: role of free radicals. Front Biosci. 2008;13:6106-25. doi: 10.2741/3141.
16. Kuroda S, Tam J, Roth JA, Sokolov K, Ramesh R. EGFR-targeted plasmonic magnetic nanoparticles suppress lung tumor growth by abrogating G2/M cell-cycle arrest and inducing DNA damage. Int J Nanomedicine. 2014;9:3825-39. doi: 10.2147/ijn.s65990.
17. El-Boubbou K. Magnetic iron oxide nanoparticles as drug carriers: clinical relevance. Nanomedicine (Lond). 2018;13(8):953-71. doi: 10.2217/nnm-2017-0336.
18. Guigou C, Lalande A, Millot N, Belharet K, Bozorg Grayeli A. Use of super paramagnetic iron oxide nanoparticles as drug carriers in brain and ear: state of the art and challenges. Brain Sci. 2021;11(3):358. doi: 10.3390/brainsci11030358.
19. Chee CF, Leo BF, Lai CW. Superparamagnetic iron oxide nanoparticles for drug delivery. In: Inamuddin, Asiri AM, Mohammad A, eds. Applications of Nanocomposite Materials in Drug Delivery. Woodhead Publishing; 2018. p. 861-903. doi: 10.1016/b978-0-12-813741-3.00038-8.
20. Kandasamy G, Sudame A, Bhati P, Chakrabarty A, Maity D. Systematic investigations on heating effects of carboxyl-amine functionalized superparamagnetic iron oxide nanoparticles (SPIONs) based ferrofluids for in vitro cancer hyperthermia therapy. J Mol Liq. 2018;256:224-37. doi: 10.1016/j.molliq.2018.02.029.

21. Jahangirian H, Kalantari K, Izadiyan Z, Rafiee-Moghaddam R, Shameli K, Webster TJ. A review of small molecules and drug delivery applications using gold and iron nanoparticles. Int J Nanomedicine. 2019;14:1633-57. doi: 10.2147/ijn.s184723.
22. Sangaiya P, Jayaprakash R. A review on iron oxide nanoparticles and their biomedical applications. J Supercond Nov Magn. 2018;31(11):3397-413. doi: 10.1007/s10948-018-4841-2.
23. Yokus B, Cakir DU, Akdag MZ, Sert C, Mete N. Oxidative DNA damage in rats exposed to extremely low frequency electro magnetic fields. Free Radic Res. 2005;39(3):317-23. doi: 10.1080/10715760500043603.
24. Amara S, Douki T, Garrel C, Favier A, Ben Rhouma K, Sakly M, et al. Effects of static magnetic field and cadmium on oxidative stress and DNA damage in rat cortex brain and hippocampus. Toxicol Ind Health. 2011;27(2):99-106. doi: 10.1177/0748233710381887.
25. Sengupta S, Balla VK. A review on the use of magnetic fields and ultrasound for non-invasive cancer treatment. J Adv Res. 2018;14:97-111. doi: 10.1016/j.jare.2018.06.003.
26. Fan Z, Hu P, Xiang L, Liu Y, He R, Lu T. A static magnetic field inhibits the migration and telomerase function of mouse breast cancer cells. Biomed Res Int. 2020;2020:7472618. doi: 10.1155/2020/7472618.
27. Yuan LQ, Wang C, Zhu K, Li HM, Gu WZ, Zhou DM, et al. The antitumor effect of static and extremely low frequency magnetic fields against nephroblastoma and neuroblastoma. Bioelectromagnetics. 2018;39(5):375-85. doi: 10.1002/bem.22124.
28. Kimsa-Dudek M, Krawczyk A, Synowiec-Wojtarowicz A, Dudek S, Pawłowska-Góral K. The impact of the co-exposure of melanoma cells to chlorogenic acid and a moderate-strength static magnetic field. J Food Biochem. 2020;44(12):e13512. doi: 10.1111/jfbc.13512.
29. Yuan LQ, Wang C, Lu DF, Zhao XD, Tan LH, Chen X. Induction of apoptosis and ferroptosis by a tumor suppressing magnetic field through ROS-mediated DNA damage. Aging (Albany NY). 2020;12(4):3662-81. doi: 10.18632/aging.102836.
30. Yang X, Song C, Zhang L, Wang J, Yu X, Yu B, et al. An upward 9.4 T static magnetic field inhibits DNA synthesis and increases ROS-P53 to suppress lung cancer growth. Transl Oncol. 2021;14(7):101103. doi: 10.1016/j.tranon.2021.101103.
31. Giorgi G, Del Re B. Epigenetic dysregulation in various types of cells exposed to extremely low-frequency magnetic fields. Cell Tissue Res. 2021;386(1):1-15. doi: 10.1007/s00441-021-03489-6.
32. Anand A, Iyer BR, Ponnusamy C, Pandiyan R, Sugumaran A. Design and development of lomustine loaded chitosan nanoparticles for efficient brain targeting. Cardiovasc Hematol Agents Med Chem. 2020;18(1):45-54. doi: 10.2174/1871525718666200203112502.
33. Shinwari Z, Al-Hindi H, Al-Shail E, Khafaga Y, Al-Kofide A, El-Kum N, et al. Response of medulloblastoma cells to vincristine and lomustine: role of TRKC, CTNNB1 and STK15. Anticancer Res. 2011;31(5):1721-33.
34. Lin KI, Lin CC, Chen MF, Chen CH, Shiu LY. Carnosic acid induces cell cycle arrest of B16F10 cells and synergizes with carmustine and lomustine in vitro and in vivo. Cancer Res. 2016;76(14 Suppl):2739. doi: 10.1158/1538-7445.am2016-2739.